

Methoxy-substituted benzo[*b*]naphtho[2,1-*d*]thiophenes and their properties relevant for optoelectronic applications

Polina A. Yaltseva, Andrey V. Khoroshutin, Anna A. Moiseeva, Sergei D. Tokarev, Vladislav M. Eliseev, Alexey E. Aleksandrov, Alexey R. Tameev, Alexander V. Anisimov, Yury V. Fedorov and Olga A. Fedorova

Table of Contents

General Information	S1
1. Synthesis.....	S2
2. NMR spectra.....	S5
3. UV-Vis and fluorescence	S8
4. Redox measurements.....	S9
5. Spectroelectrochemistry measurements	S11
6. Frozen matrix phosphorescence	S12
7. Charge carriers measurements.....	S12
References	S14

General Information

NMR spectra are registered on Bruker Avance-400 instrument (400.13 and 125.13 MHz for ¹H and ¹³C, respectively). Chemical shifts are reported with respect to that of the residual proton chemical shift and that of carbon-13 signals of the solvent (7.27 ppm for and 77.0 ppm of ¹³C in CDCl₃). High resolution mass spectra have been recorded at Bruker Maxis Impact and Thermo Scientific LTQ instruments^{S1}. Photochemical reactions have been carried out in the reactor with a thermostated quartz well immersed into a reaction mixture; the low pressure 120W Hg lamp was placed into the well.

TLC control of the reactions was performed with the plates "Silica gel on TLC Al foils 60 F254 Sigma Aldrich" и "DC-Alufolien Aluminiumoxid 60 F254 neutral Merck". Column chromatography has been done with Silica Gel 60 (particle size 0.063-0.2 mm, Merck) and with aluminium oxide LC90 Å (particle size 0.063-0.2 mm, Macherey-Nagel).

Absorption and fluorescence spectra have been measured on Varian Cary-300 and Varian Cary Eclipse, respectively. Fluorescence spectra have been measured at 20 ± 1 °C and are corrected. Quantum yield was measured with respect to quinine sulfate in 1N H_2SO_4 . ^{S2}

Redox experiments were done in house-made 3- electrode electrochemical cell, glass carbon electrode (d=2 mm) used as working electrode, Pt as counter electrode, $\text{Ag}/\text{AgCl}/\text{KCl}_{\text{aq. sat.}}$ as the reference electrode connected to the cell *via* salt bridge. Measured Fc/Fc^+ potential was 0.48 V.

Luminescence at 77 K and luminescence decay was recorded with FluoroLog-3-221 (Horiba Scientific). Xe-lamp in pulse mode (3 μs) was used. 10^{-3}M solution in MeCN was placed to a glass tube (inner diameter 2 mm), the tube then was placed to a liquid-N₂ –cooled quartz Dewar flask equipped with optical quartz windows. Emission was detected in the front mode. Position of all the sample setup in the optical compartment was tuned manually to ensure maximum signal. Luminescence decay was registered by measuring the luminescence intensity dependence on the delay (10 μs and longer) after the excitation pulse.

Spectroelectrochemistry experiments were performed at 22 °C with a Metrohm Autolab B.V. potentiostat. Compounds were dissolved in DMF containing NBu_4PF_6 as the supporting electrolyte (0.1 M). Dry argon gas was bubbled through the solutions for 10 min before experiments. Honeycomb Spectroelectrochemistry Cell Kit was used as electrochemical cell. Platinum Honeycomb Spectroelectrochemical Electrode Chip included in the Kit contains an onboard working Pt, counter and reference electrode so no additional components were needed. Changes in UV-Vis absorption spectra upon applying potentials were recorded by Avantes AvaSpec-2048 spectrophotometer.

Molecular structures were optimized by Gaussian'09 program^{S3} with the specified basis.

Solvents have been purified according to standard procedures. ^{S4}

1. Synthesis

3-Methylbenzothiophene^{S5} **3**, 3-(bromomethyl)benzothiophene^{S6} were synthesized according to the known procedures.

Diethyl (1-benzothien-3-ylmethyl)phosphonate (4) Triethyl phosphite (1.881 ml, 1.825 g, 11.0 mmol) was added to 3-(bromomethyl)-1-benzothiophene (2.05 g, 9.03 mmol), and the reaction mixture was heated at 160 °C for 8 h. The mixture was placed to a sublimation apparatus with the cooling finger equipped with a little cup for the liquid collection. Admixtures were sublimed off in a vacuum of 0.15 Torr when the apparatus was heated at 140 °C with an oil bath. The residue consisted in the target phosphonate, 90% purity. The phosphonate was used in further reaction as is, taking into account the amount of admixtures. Isolated yield 1.02 g. ¹H

¹H NMR: (CDCl₃, δ, ppm, J Hz): 1.17 (t, 6H, ³J = 7.0), 3.42 (dd, 2H, ²J_{P-H} = 21.2, ⁴J_{H-H} = 0.9), 3.92-4.03 (m, 4H), 7.31-7.40 (m, 3H), 7.78-7.83 (m, 2H).

3-[*(E*)-2-(4-Methoxyphenyl)ethenyl]benzo[*b*]thiophene (5) ⁵⁷ Dispersion of NaH (60%) in mineral oil (63.6 mg, 1.59 mmol, 4-fold excess) was dissolved in DME (7 ml). A solution of diethyl (1-benzothien-3-ylmethyl)phosphonate **3** (150 mg, 0.53 mmol) in DME (1 ml) was added in small portions at 0 °C. After stirring for 15 min, a solution of *p*-methoxybenzaldehyde (72 mg, 0.53 mmol) in DME (1 ml) was added in small portions. The reaction mixture was allowed to warm to room temperature and stirred for 5 h. The reaction mixture has been added to cold water (50 ml). The precipitate formed was filtered off and recrystallized from petroleum ether. Recrystallization afforded **5** (126 mg, 0.47 mmol, 89%). ¹H NMR (400 MHz, CDCl₃, δ ppm, J/Hz): 3.86 (s, 3H), 6.94 (d, 2H, ³J = 8.8), 7.15 (d, 1H, ³J = 16.3), 7.28 (d, 1H, ³J = 16.3), 7.37-7.47 (m, 2H), 7.50-7.53 (m, 3H), 7.87 (d, 1H, ³J = 7.5), 8.01 (d, 1H, ³J = 7.5).

3-[*(E*)-2-(3,5-Dimethoxyphenyl)ethenyl]benzo[*b*]thiophene (6)

A dispersion of NaH (60%) in mineral oil (63.6 mg, 1.59 mmol, 4.5-fold excess) was dissolved

in DME (7 ml). A solution of diethyl (1-benzothien-3-ylmethyl)-phosphonate **3** (100 mg, 0.53 mmol) in DME (1 ml) was added in small portions at 0 °C. After stirring for 15 min, a solution of 3,5-dimethoxybenzaldehyde (58 mg, 0.35 mmol) in DME (1 ml) was added in small portions. The reaction mixture was allowed to warm to room

temperature and stirred for 5 h. The mixture was added to cold water (50 ml). The precipitate formed was filtered off and recrystallized from petroleum ether. Recrystallization afforded **6** (80 mg, 0.269 mmol, 77%). ¹H NMR (400 MHz, CDCl₃, δ ppm, J/Hz): 3.86 (s, 6H, -OCH₃), 6.43 (t, 1H, ⁴J = 2.2, H(15)), 6.72 (d, 2H, ⁴J = 2.2, H(13,17)), 7.13 (d, 1H, ³J = 16.3, -CH=CH-), 7.35-7.48 (m, 3H, H(8,7), -CH=CH-), 7.58 (s, 1H, H(2)), 7.89 (d, 1H, ³J = 7.7, H(6 or 9)), 8.02 (d, 1H, ³J = 7.7, H(9 или 6)). ¹³C NMR (100 MHz, CDCl₃, δ ppm): 161.0, 140.5, 139.4, 137.7, 133.9, 130.2, 124.6, 124.3, 122.9, 122.1, 121.9, 121.2, 104.5, 100.0, 55.4. HRMS m/z: 297.0950 [M + H]⁺; Calcd: C₁₇H₁₂OS 297.0944

2-Methoxy[*b*]naphtho[2,1-*d*]thiophene (1). 3-[(*E*)-2-(4-Methoxyphenyl)ethenyl]-benzo[*b*]thiophene **5** (53 mg, 0.19 mmol) was dissolved in benzene (100 ml), then iodine (51 mg, 0.2 mmol) has been added to the solution. The solution was placed into the photoreactor, the solution was purged with argon for 15 min. Then propylene oxide (2.8 ml, 2.3 g, 40 mmol) was added and the lamp was turned on. The solution was irradiated for 4 h at constant argon flow; propylene oxide (1 ml, 830 mg, 14 mmol) was added every hour. The solution was evaporated, and the residue was purified by column chromatography (SiO₂, petroleum ether-ethyl acetate 20:1) to afford 32 mg (0.12 mmol, 64%) of product **1**. ¹H NMR (400 MHz, CDCl₃, δ ppm, J/Hz):

3.97 (s, 3H, -OCH₃), 4.15 (s, 3H, -OCH₃), 6.69 (d, 1H, ⁴J=2.2 Hz, H(15) or H(17)), 6.96 (d, 1H, ⁴J=2.2 Hz, H(15) or H(17)), 7.44-7.53 (m, 2H, H(4,5)), 7.75 (d, 1H, 3J = 8.6, H(13) or H(12)), 7.96-7.98 (m, 1H, H(3) or H(6)), 8.20-8.23 (m, 2H, H(6) or H(3), H(12) or H(13)). ¹³C NMR (100 MHz, CDCl₃, δ ppm): 55.08, 55.33, 97.83, 99.24, 116.69, 120.29, 120.38, 121.85, 123.60, 124.90, 128.57, 130.44, 133.75, 134.52, 134.71, 139.87, 156.19, 157.78. HRMS m/z: 264.0606 [M⁺]; Calcd: C₁₇H₁₂OS 264.0603

1,3-Dimethoxy[*b*]naphtho[2,1-*d*]thiophene (2). 3-[(*E*)-2-(3,5-Dimethoxyphenyl)-ethenyl]benzo[*b*]thiophene **6** (53 mg, 0.19 mmol) was dissolved in benzene (100 ml), then iodine (51 mg, 0.2 mmol) was added to the solution. The solution was placed into the photoreactor, the solution was purged with argon for 15 min. Then propylene oxide (2.8 ml, 2.3 g, 40 mmol) was added, and the lamp was turned on. The solution was irradiated for 4 h at constant argon flow; propylene oxide (1 ml, 830 mg, 14 mmol) was added every hour. The solution was evaporated, and the residue was purified by column chromatography (SiO₂, petroleum ether-ethyl acetate 20:1) to afford 20 mg (0.068 mmol, 38%) of product **2**. ¹H NMR (400 MHz, CDCl₃, δ ppm, J/Hz): 3.97 (s, 3H, -OCH₃), 4.15 (s, 3H, -OCH₃), 6.69 (d, 1H, ⁴J=2.2 Hz, H(15) or H(17)), 6.96 (d, 1H, ⁴J=2.2 Hz, H(15) or H(17)), 7.44-7.53 (m, 2H, H(4,5)), 7.75 (d, 1H, 3J = 8.6, H(13) or H(12)), 7.96-7.98 (m, 1H, H(3) or H(6)), 8.20-8.23 (m, 2H, H(6) or H(3), H(12) or H(13)). ¹³C NMR (100 MHz, CDCl₃, δ ppm): 55.08, 55.33, 97.83, 99.24, 116.69, 120.29, 120.38, 121.85, 123.60, 124.90, 128.57, 130.44, 133.75, 134.52, 134.71, 139.87, 156.19, 157.78 . HRMS m/z: 294.0708 [M⁺]; Calcd: C₁₇H₁₂OS 294.0709.

2. NMR spectra

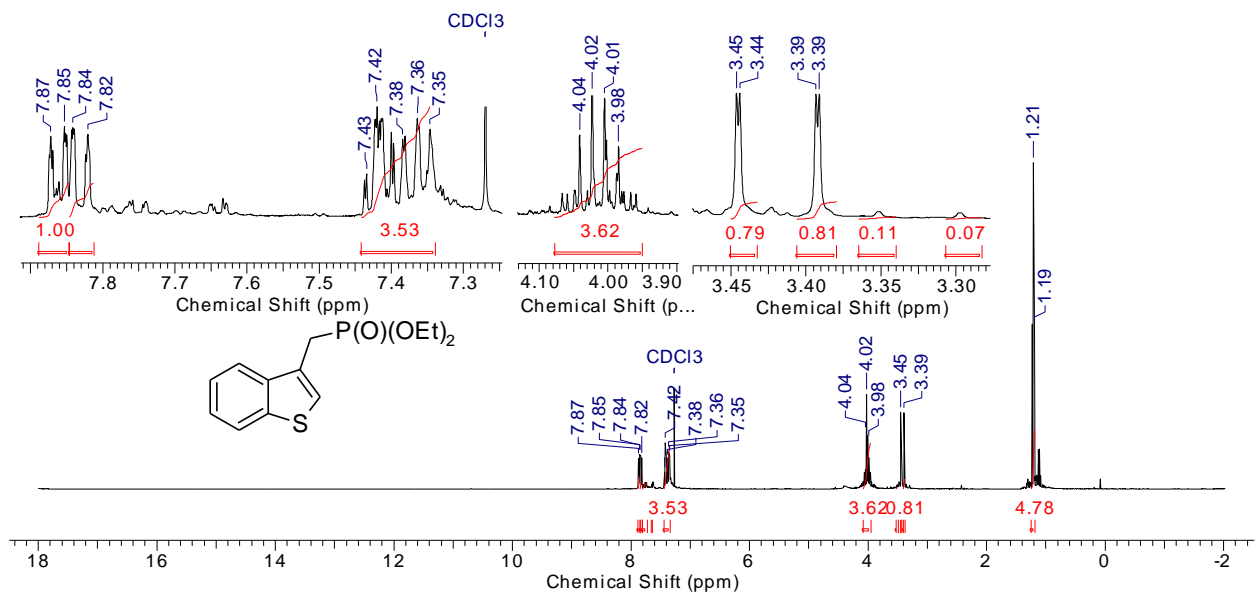


Figure S1. ^1H NMR of diethyl (1-benzothien-3-ylmethyl)phosphonate

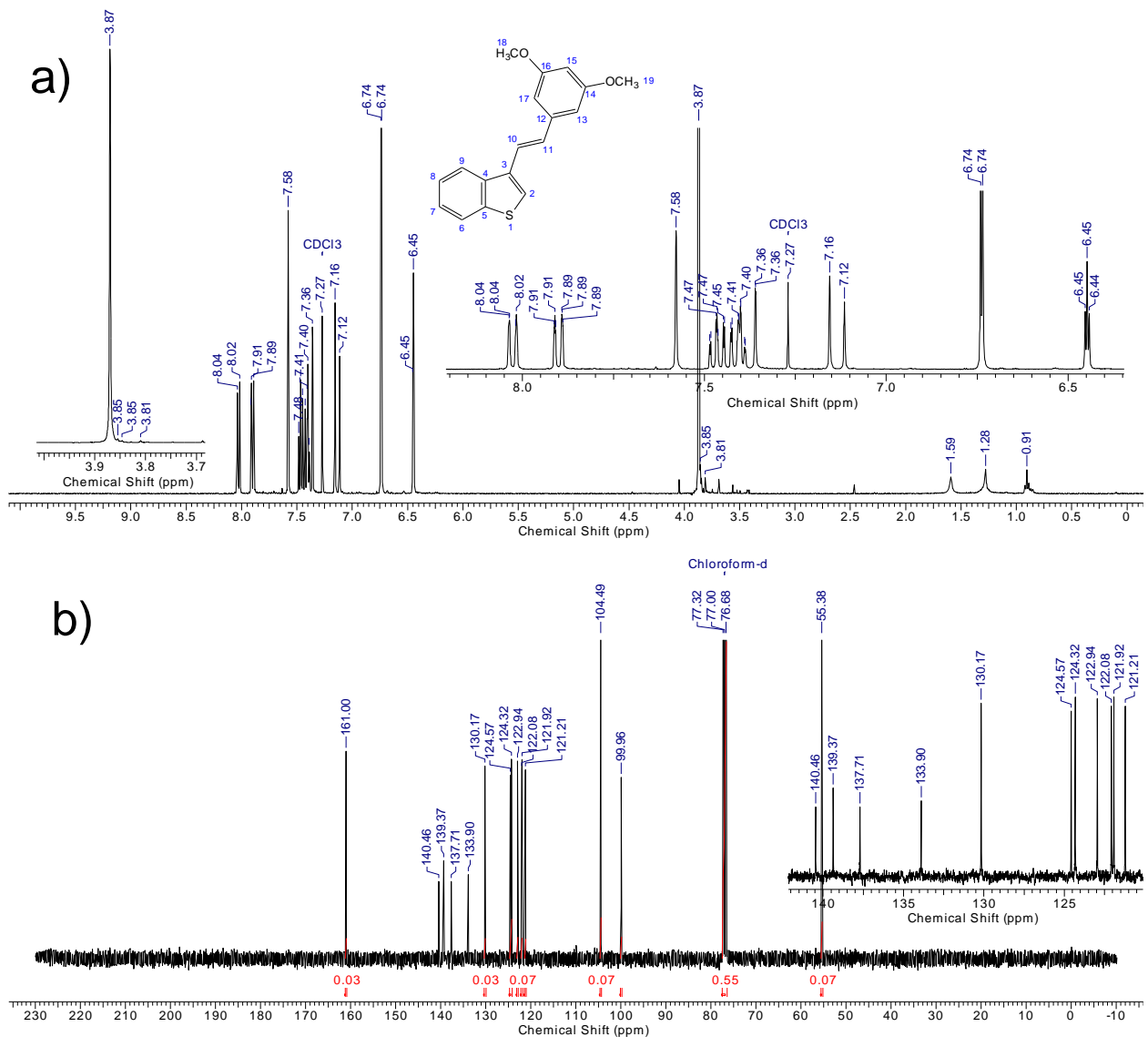


Figure S2. ^1H (a) and ^{13}C (b) NMR of 3-[(E)-2-(3,5-dimethoxyphenyl)ethenyl]-benzo[b]thiophene.

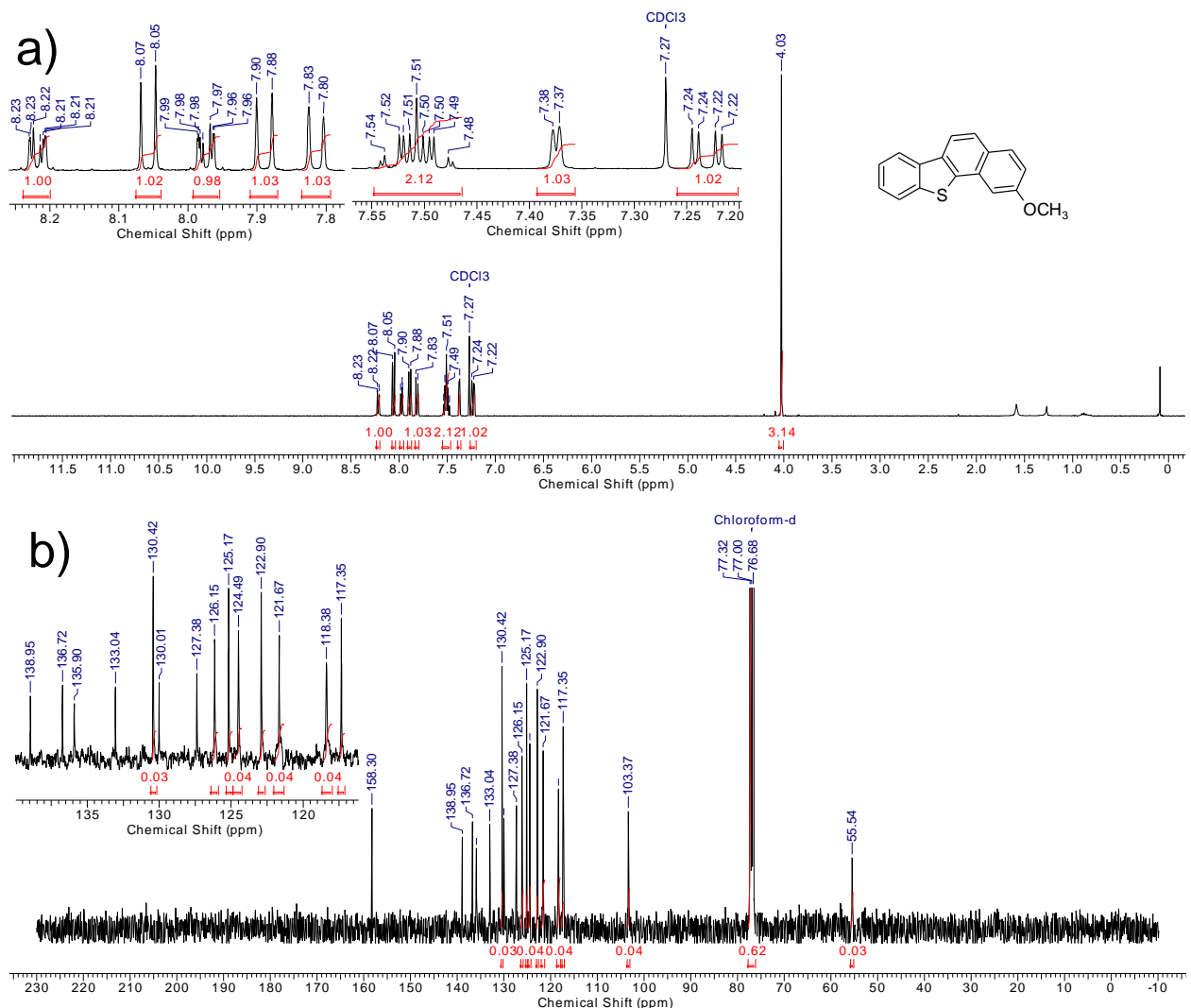


Figure S3. ^1H (a) and ^{13}C (b) NMR of 2-methoxybenzo[*b*]naphtho[2,1-*d*]thiophene

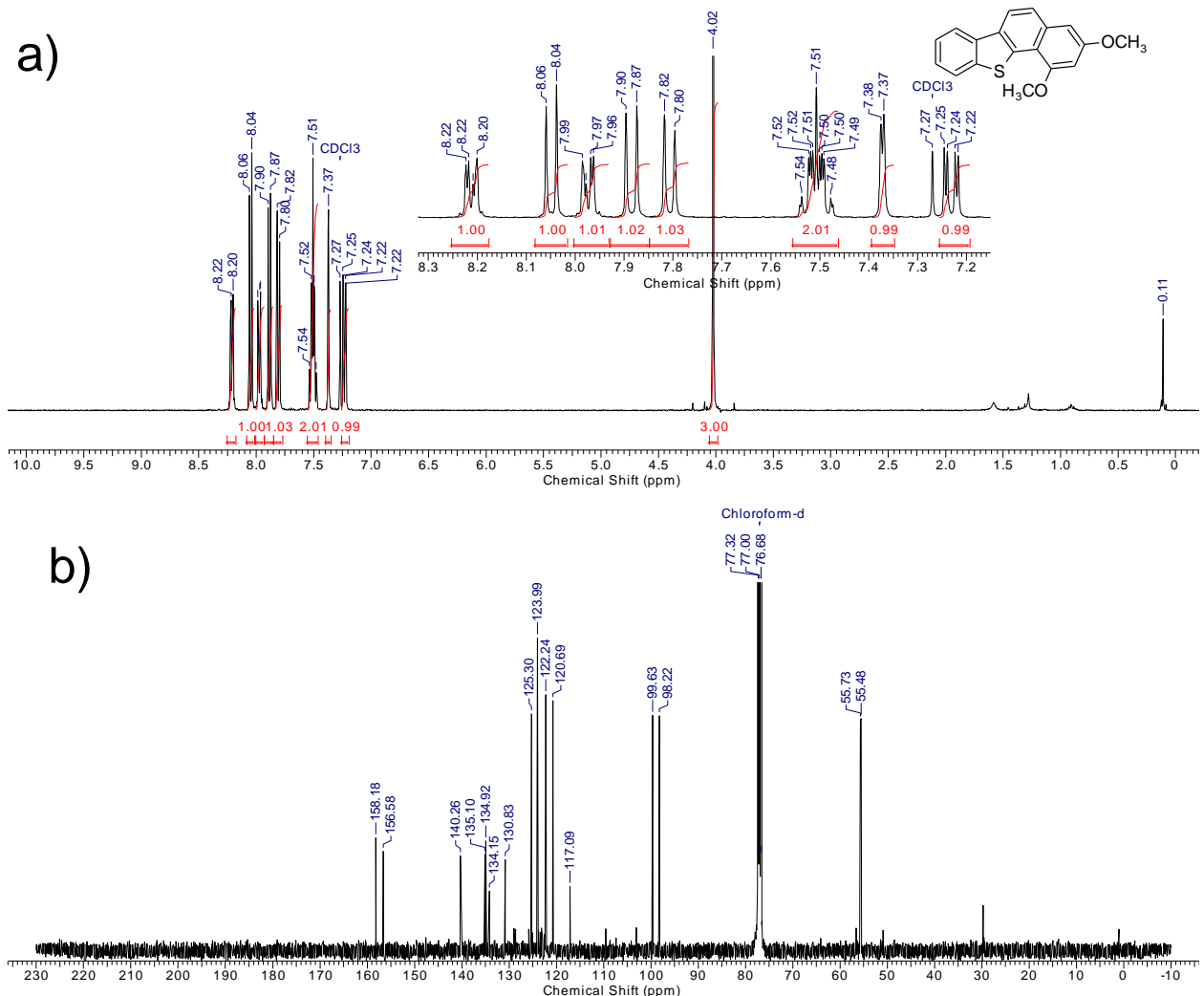


Figure S4. ^1H (a) and ^{13}C (b) NMR of 1,3-dimethoxybenzo[*b*]naphtho[2,1-*d*]thiophene

3. UV-Vis and fluorescence

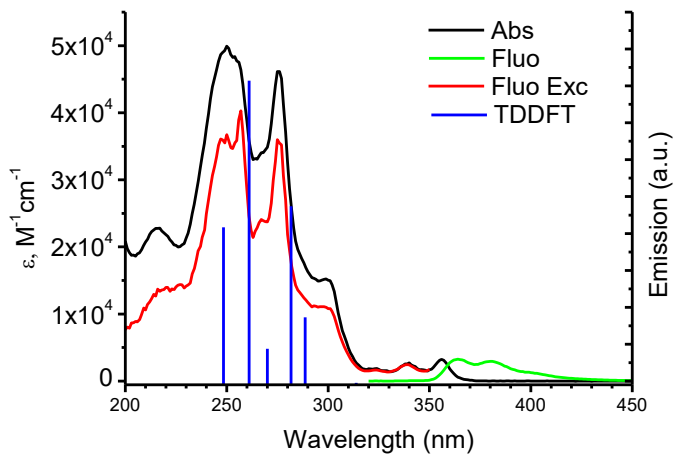


Figure S5. UV-Vis (5×10^{-5} M, MeCN), fluorescence ($\lambda_{\text{exc}}=310$ nm), fluorescence excitation ($\lambda_{\text{emis}}= 360$ nm) of **1**. TD-DFT spectra (8 singlet and 8 triplet states; B3LYP/6-31+g(d))

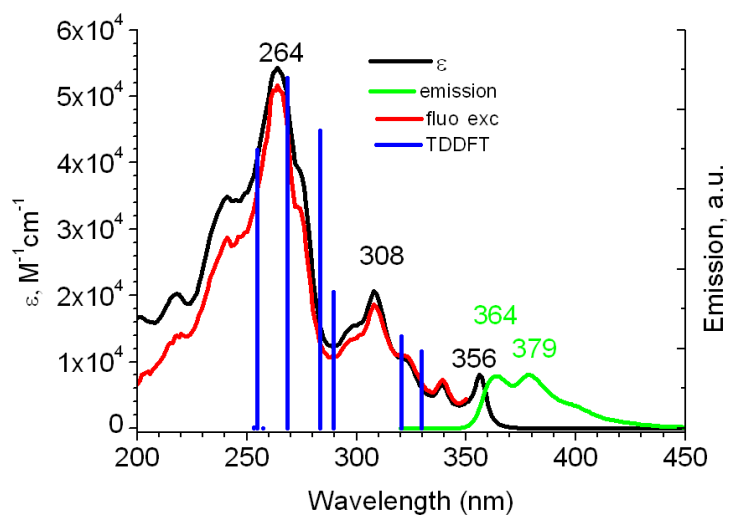


Figure S6. UV-Vis (5×10^{-5} M, MeCN), fluorescence ($\lambda_{\text{exc}} = 310$ nm), fluorescence excitation ($\lambda_{\text{emis}} = 360$ nm) of **2**. TD-DFT spectra (8 singlet and 8 triplet states; B3LYP/6-31+g(d))

4. Redox measurements

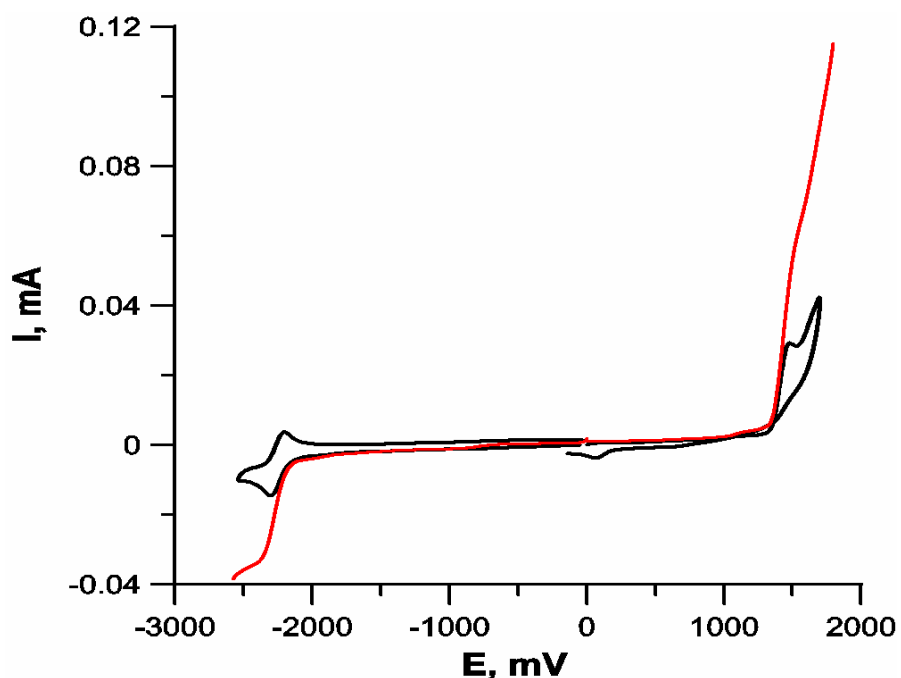


Figure S7. Cyclic voltammetry (CVA, black) and rotating disc electrode (RDE, red) curves measured for **1**, 10^{-3} M solution in DMF, 0.1 M TBAP used as the supporting electrolyte. Potentials are reported with respect to Ag/AgCl/KCl_{aq,sat}; connected via the salt bridge, Fc/Fc⁺ 0.48 V.

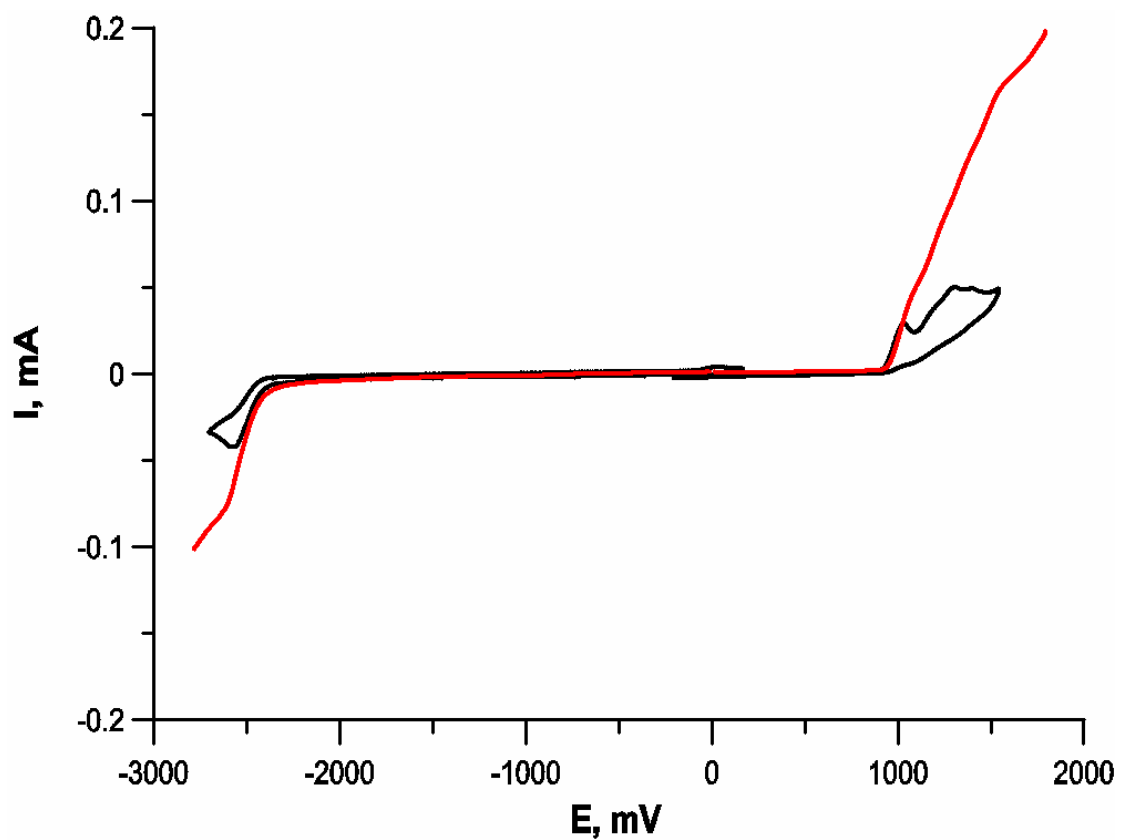


Figure S8 . Cyclic voltammetry (CVA, black) and rotating disc electrode (RDE, red) curves measured for **2**, 10^{-3} M solution in DMF, 0.1 M TBAP used as the supporting electrolyte. Potentials are reported with respect to Ag/AgCl/KCl_{aq,sat}; connected *via* the salt bridge, Fc/Fc⁺ 0.48 V.

5. Spectroelectrochemistry measurements

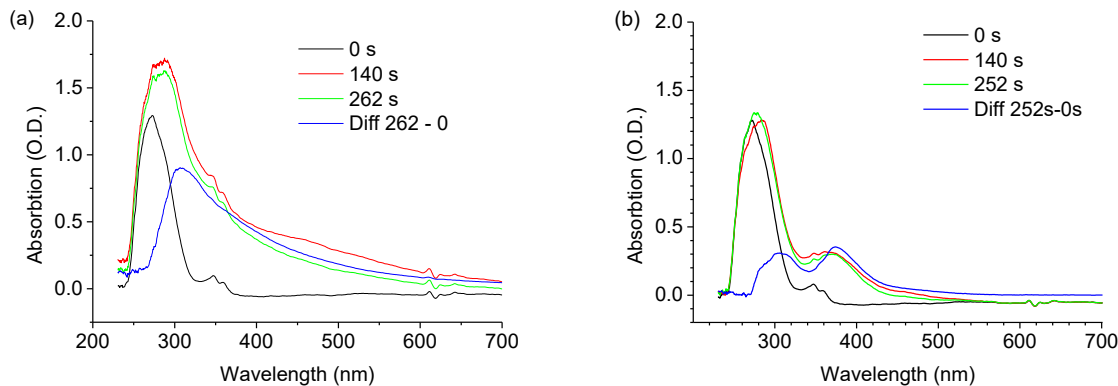


Figure S9. UV-Vis spectra evolution experiments for (a) -2.35 V and (b) 1.7V potentials.

$C\ 6.4 \times 10^{-3} M$; $NBu_4PF_6 - 10^{-1} M$. Potential profile: 0 V(20 s) \rightarrow 1.7(a) or -2.35 V (b) (140 s) \rightarrow 0 V (rest of the experiment)

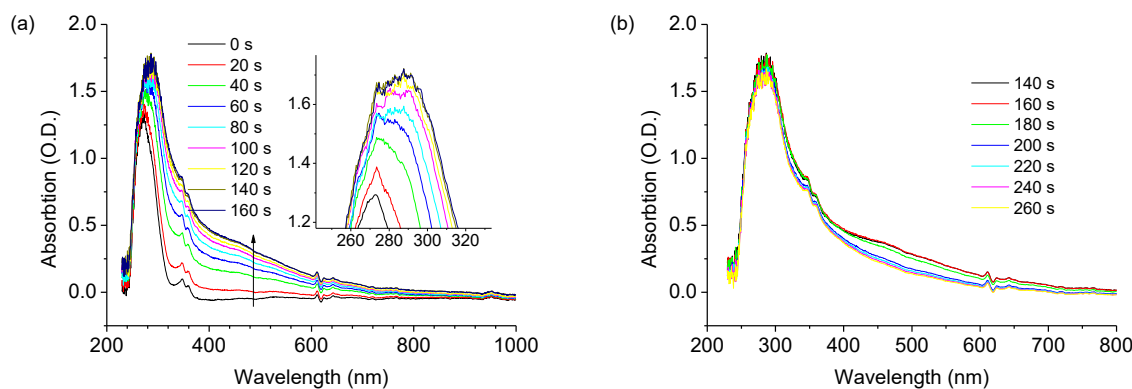


Figure S10 . Evolution of UV-Vis spectrum of **1** when (a) -2.35 V is applied at working electrode and (b) potential is set back to 0 V

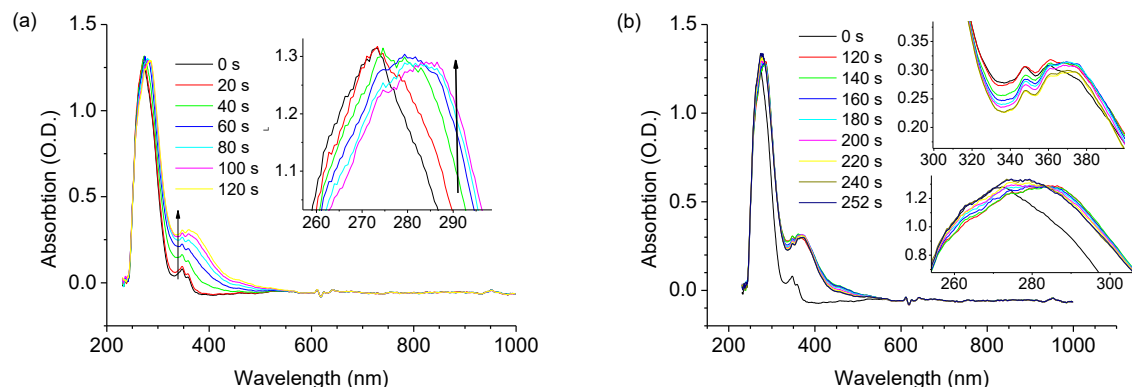


Figure S11 . Evolution of UV-Vis spectrum of **1** when (a) 1.75 V is applied at working electrode and (b) potential is set back to 0 V

6. Frozen matrix phosphorescence

Luminescence at 77 K and luminescence decay was recorded by FluoroLog-3-221 (Horiba Scientific). Xe-lamp in pulse mode (3 μ s) was used. A 10⁻³ M solution in MeCN was placed to a glass tube (inner diameter 2 mm), the tube then was placed to a liquid-N₂ –cooled quartz Dewar flask equipped with optical quartz windows. Emission was detected in the front mode. Position of all the sample setup in the optical compartment was tuned manually to ensure maximum signal. Luminescence decay was registered by measuring the luminescence intensity dependence on the delay (10 μ s and longer) after the excitation pulse.

7. Charge carriers measurements

To access the applicability of the studied systems for organic semiconductor applications we did the measurements of charge carriers mobilities by CELIV method (current extraction with a linear increase in voltage) method.⁸⁸ 5 mm Layer of **1** obtained by drop cast exhibited the following charges mobilities $\mu_e = 0.249 \text{ cm}^2 \text{V}^{-1} \text{s}^{-1}$ and $\mu_h = 0.198 \text{ cm}^2 \text{V}^{-1} \text{s}^{-1}$.

The layout of the photo-CELIV installation and the architecture of the device are shown in Figure S12. The device is a flat capacitor with a layer under study between two electrodes, the one of them is a blocking one. The sample was prepared as follows. A 70 nm thick layer of SiO₂ was deposited by magnetron sputtering on a glass substrate (20 \times 30 mm \times mm) with an ITO electrode (KAIKO[®], 7 $\Omega \text{ m}^{-2}$). After that, a layer of compound **1** was applied from a solution in *m*-xylene at a concentration of 10 mg ml⁻¹. The layer thickness was 5 μm . An aluminum layer with a thickness of 100 nm was thermally sputtered on the top from above through the mask under a pressure below 10⁻⁵ mbar in an Auto 500 evaporator (EDWARDS) coupled to a glove box (MBraun) with an Ar atmosphere. The top four electrodes had an area of 13.8 mm².

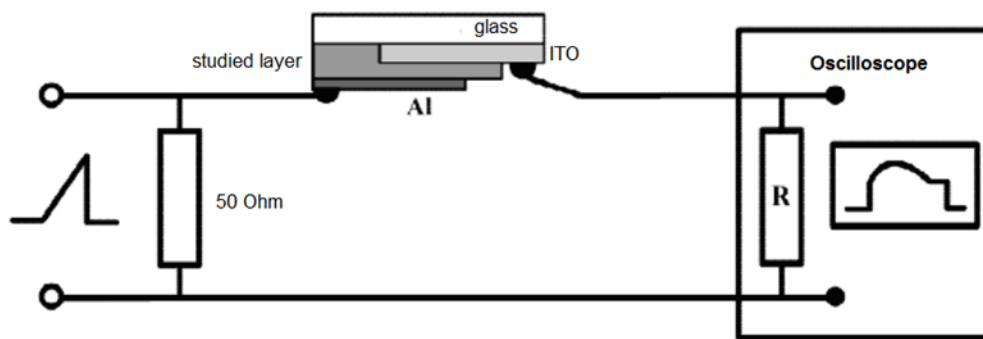


Figure S12. Schematic representation of a photo-CELIV experimental setup and a device architecture.

In devices, the SiO₂ dielectric layer served as a layer blocking the injection of both holes and electrons from the ITO electrode into the active layer. To measure the electron mobility, a

negative bias was applied to the aluminum electrode. As a result, electrons were accumulated at the interface between the SiO_2 layer and the active layer, and then they were extracted using a linearly increasing triangular voltage pulse.

Similarly, but with the positive bias at the Al electrode, holes were accumulated at SiO_2 . The voltage rise rate A varied in the range from 1×10^4 to $8 \times 10^5 \text{ V s}^{-1}$. To increase the charge carrier concentration (*i.e.*, the transient current signal), the active layer was irradiated through the glass/ITO electrode with a 405 nm / 1 μs laser pulse 1 μs before bias was applied. The photo-CELIV experiments were carried out in the argon-filled glove box. The transient currents were measured across the load resistor R of a DL-Analog Discovery oscilloscope (Digilent Co.) (Fig. S12). A typical transient signal is shown in Figure S13.

At the transient current, the time to peak the extraction current, t_{\max} , was used to calculate the drift mobility, μ , according to the equation:

$$\mu = \frac{2d^2}{3At_{\max}^2}$$

It is valid for the transport of charge carriers generated in the bulk, provided that the conduction current is less than capacitance current ^{S8a, S9}, so registered photo-CELIV currents correspond well to the expression.

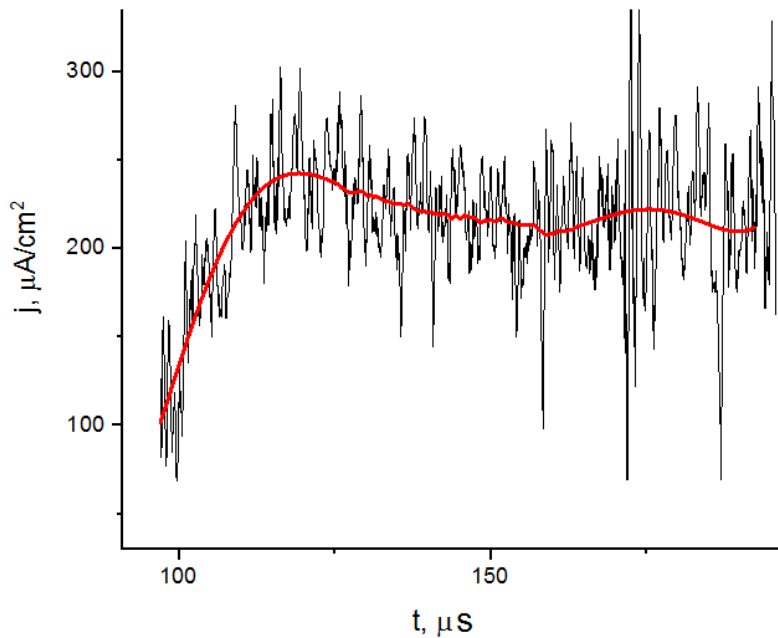


Figure S13. CELIV current of holes for the ITO/ SiO_2 /1/Al device.

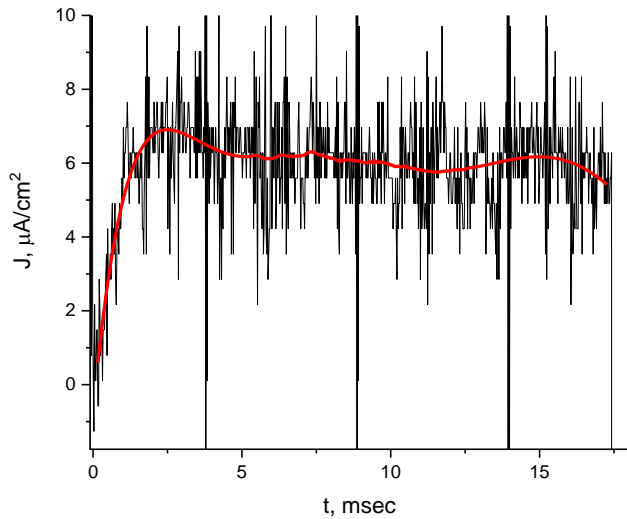


Figure S14. CELIV current of holes for the ITO/SiO₂/2/Al device.

References

S1 P. A. Belyakov, V. I. Kadentsev, A. O. Chizhov, N. G. Kolotyrkina, A. S. Shashkov and V. P. Ananikov, *Mendeleev Commun.*, 2010, **20**, 125.

S2 J. R. Lakowitz, *Principles of Fluorescence Spectroscopy*, Springer, Singapore, 2006.

S3 M. J. Frisch, G. W. Trucks, H. B. Schlegel, G. E. Scuseria, M. A. Robb, J. R. Cheeseman, G. Scalmani, V. Barone, B. Mennucci, G. A. Petersson, H. Nakatsuji, M. Caricato, X. Li, H. P. Hratchian, A. F. Izmaylov, J. Bloino, G. Zheng, J. L. Sonnenberg, M. Hada, M. Ehara, K. Toyota, R. Fukuda, J. Hasegawa, M. Ishida, T. Nakajima, Y. Honda, O. Kitao, H. Nakai, T. Vreven, J. J. A. Montgomery, J. E. Peralta, F. Ogliaro, M. Bearpark, J. J. Heyd, E. Brothers, K. N. Kudin, V. N. Staroverov, T. Keith, R. Kobayashi, J. Normand, K. Raghavachari, A. Rendell, J. C. Burant, S. S. Iyengar, J. Tomasi, M. Cossi, N. Rega, J. M. Millam, M. Klene, J. E. Knox, J. B. Cross, V. Bakken, C. Adamo, J. Jaramillo, R. Gomperts, R. E. Stratmann, O. Yazyev, A. J. Austin, R. Cammi, C. Pomelli, J. W. Ochterski, R. L. Martin, K. Morokuma, V. G. Zakrzewski, G. A. Voth, P. Salvador, J. J. Dannenberg, S. Dapprich, A. D. Daniels, O. Farkas, J. B. Foresman, J. V. Ortiz, J. Cioslowski and D. J. Fox, 09, , Revision B.01 ed., Gaussian, Inc., Wallingford CT, 2010.

S4 W. L. E. Armarego and C. L. L. Chai, *Purification of Laboratory Chemicals*, 5 edn., Butterworth Heinemann, Amsterdam, 2003.

S5 *Syntheses of sulfides, thiophenes and thioles of the types found in petroleum (Sintez sul'fidov, tiofenov i tiolov, vstrechayushchikhsya v neftyakh)* ed. E. N. Karaulova, Nauka, Moscow, 1988.

S6 A. de Dios, L. Prieto, J. A. Martín, A. Rubio, J. Ezquerra, M. Tebbe, B. López de Uralde, J. Martín, A. Sánchez, D. L. LeTourneau, J. E. McGee, C. Boylan, T. R. Parr and M. C. Smith, *J. Med. Chem.*, 2002, **45**, 4559.

S7 N. Pentala, P. Crooks, V. Sonar and N. R. Pentala, 2014, 76.

S8 (a) G. Juska, K. Arlauskas, M. Viliunas, K. Genevicius, R. Osterbacka and H. Stubb, *Phys. Rev. B*, 2000, **62**, R16235; (b) O. Grynko, G. Juška and A. Reznik, in *Photoconductivity and Photoconductive Materials*, (Ed.: S. O. Kasap), John Wiley & Sons, 2022, pp. 339.

S9 M. Stephen, K. Genevicius, G. Juska, K. Arlauskas and R. C. Hiorns, *Polym. Int.*, 2017, **66**, 13.